

JAERI-M

5 6 4 9

ANOMALOUS PLASMA LOSS IN THE JAERI
TOROIDAL HEXAPOLE

February 1974

H. OHTSUKA, S. TAMURA, T. NAGASHIMA
T. SHIINA, H. YAMATO and S. ARIZONO

日 本 原 子 力 研 究 所
Japan Atomic Energy Research Institute

この報告書は、日本原子力研究所が JAERI-M レポートとして、不定期に刊行している研究報告書です。入手、複製などのお問い合わせは、日本原子力研究所技術情報部（茨城県那珂郡東海村）あて、お申しこしください。

JAERI-M reports, issued irregularly, describe the results of research works carried out in JAERI. Inquiries about the availability of reports and their reproduction should be addressed to Division of Technical Information, Japan Atomic Energy Research Institute, Tokai-mura, Naka-gun, Ibaraki-ken, Japan.

Anomalous Plasma Loss in the JAERI Toroidal Hexapole

Hidewo OHTSUKA, Sanae TAMURA, Takashi NAGASHIMA,

Tomio SHIINA, Harumi YAMATO* and Shigeki ARIZONO

Thermonuclear Fusion Lab., Tokai, JAERI

(Received February 12, 1974)

Anomalous plasma loss in the JAERI hexapole has been investigated, with emphasis on a field error due to induced wall current and on a support induced convection. The field error produced by the inhomogeneous wall current has no large influence on the plasma confinement. The supports cause plasma loss by way of a convective flow, besides the direct loss.

* On leave from the Research and Development Center, Tokyo Shibaura Electric Co., Ltd. Kawasaki, Japan.

原研トロイダルヘクサポールにおける
プラズマの異常損失機構

日本原子力研究所東海研究所核融合研究室

大塚英男，田村早苗，永島 孝
椎名富雄，大和春海，有蘭重喜

(1974年2月12日受理)

原研トロイダルヘクサポール型プラズマ閉じ込め装置におけるプラズマの損失機構を調べた。装置の壁を流れる誘導電流がもたらす不整磁場によるものと，内部導体を支持するサポートによるものの二つに特に注目した。実験の結果以下の事が明らかになった。

① 壁電流による不整磁場はプラズマ損失の主な原因とはなっていない。② サポートは直接的な損失源ばかりでなく，対流による損失をおこす原因となっている。

目 次 な し

I. Introduction

Confinement experiments have been made in the JAERI toroidal hexapole¹ (JFT-1) putting emphasis on investigation of plasma loss processes. In a previous experiment made with an additional error field, plasma convection due to added error field was observed.² This suggests that the intrinsic error magnetic field of the device can possibly be a cause of the observed anomalous loss¹ in JFT-1 by inducing convective flows in the plasma. The intrinsic magnetic perturbation in JFT-1 has mainly been ascribed to azimuthal nonuniformity of the induced wall currents; disturbance in the wall currents due to various large portholes of the vacuum chamber produces error magnetic fields large enough in magnitude ($\Delta B/B \sim 1\%$) to destroy the azimuthal symmetry of the confining magnetic field. An azimuthally symmetric conducting shell was installed inside the vacuum chamber to improve the azimuthal uniformity of the wall currents and thereby to reduce the error magnetic fields. At the same time, the outer hoops were replaced by new ones of smaller cross-section to increase the available magnetic flux around them. In section II, experimental results obtained in this new arrangement are described in comparison with previous results.

Another possible cause of the observed anomalous loss is an obstacle-induced plasma convection. Since our device has twenty rod supports in total, these supports will probably induce azimuthal inhomogeneity in plasma potentials, and this may cause enhancement of plasma loss by forming convective flows of plasma. In order to study the effect of the existing supports experimentally, a model support was introduced into the plasma and the subsequent changes in the plasma potential and the density were investigated. This experiment is described in section III. A similar experiment has been made in the Wisconsin octupole^{3,4} and is compared with the present experiment in section IV. The anomalous plasma loss mechanisms in JFT-1 are also discussed in section IV on the basis of the present experiment.

II. Effect of an azimuthally symmetric shell

A cross-sectional view of the device for the present experiment is shown in Fig. 1. An aluminum shell with contoured inner surface was installed inside the vacuum chamber and the minor diameter of the outer hoops was reduced to 32 mm (previously 42 mm). Measurements of magnetic field pattern were made using an electron beam, but detailed structure of

the flux configuration was not obtainable due to restriction in accessibility imposed by the shell. The effect of the shell therefore was studied by measurements of overall plasma properties. The effect of the reduction of the outer hoop cross-section may also be included in the present experimental results.

The experiment was made with microwave-produced hydrogen plasma with density, $n \sim 4 \times 10^{10} \text{ cm}^{-3}$, and electron temperature, $T_e \sim 0.6 \text{ eV}$. Langmuir probes were used to measure the electron temperature and the plasma density. The plasma loss to the hoops and the walls was measured using flux collecting limiter-detectors. The average magnetic field strength is typically about 900 G on the stability limit line.

Figure 2 shows azimuthal variations of loss fluxes to the outer hoop. The azimuthal profile changes by the reversal of the polarity of the magnetic field. This shows there still exists an azimuthal inhomogeneity in plasma loss fluxes; if these azimuthal variations of loss fluxes are due to some arrangement errors of detectors, they should not depend on the magnetic field polarity. Since the measurement was made at only six points in the azimuthal direction, it is difficult to locate some disturbance source from this profile. Measurements of plasma loss to the wall also show inhomogeneity in the azimuthal direction similar to the loss to the hoop. The confinement time estimated from the relation, $\tau = \left(\frac{1}{N} \frac{dN}{dt}\right)^{-1}$, is shown in Fig. 3 (a) in comparison with the previous results, where N is the average plasma density. No appreciable change in the overall confinement time is observed. If we assume that no support is present in the plasma, the confinement time will be given by $\tau_{\perp} = N/\Gamma_{\perp} = \tau (1 + \Gamma_{\parallel}/\Gamma_{\perp})$, where Γ_{\parallel} and Γ_{\perp} are the parallel and the perpendicular loss flux, respectively. As shown in Fig. 3 (b), slight improvement in τ_{\perp} is observed. Effective diffusion coefficients $\langle D \rangle$ in the three typical regions of the hexapole are shown in Fig. 4 together with the previous results, where $\langle D \rangle$'s are calculated from the measured loss fluxes and the density gradients using the relation $\Gamma_{\perp} = \langle D \rangle \frac{dn}{dx}$. While almost no change is observed in $\langle D \rangle$'s near the inner hoop and the wall, considerable decrease in $\langle D \rangle$ results near the outer hoop. Figure 5 shows the fraction of the plasma losses in different directions as a function of magnetic field strength. The result of the present experiment shows that the fractional loss to the hoop is considerably decreased as the magnetic field strength is increased.

As mentioned previously, the experimental results described above include combined effects of the shell and the reduction of the cross-section of the outer hoop, and it is rather difficult to single out the effect of the shell, or the influence of the error field due to inhomogeneous wall currents on the plasma confinement. Nevertheless the experimental results obtained here may be summarized as follows: (i) Since almost no improvement has been obtained in the azimuthal distribution of the perpendicular loss fluxes and in the confinement time τ , it may be said that the error field of the type discussed here has no major influence on the plasma confinement in JFT-1; (ii) Considerable decrease compared with the previous results has been observed in the plasma loss to the outer hoop, and "anomaly" observed in the effective diffusion coefficient near the outer hoop has disappeared as shown in Fig. 4. Slight increase in τ has resulted due mainly to the decrease in the loss flux to the outer hoop. These results may be closely related to the increase in the magnetic flux around the outer hoop, but physical processes involved have not been made clear.

III. Support-induced convection

The experimental arrangement is shown in Fig. 6. The model support used in this experiment is 10 mm-diam. stainless steel rod, and is introduced into the same high-field region as the real supports of the outer hoop. Local co-ordinates (X , Z) are used to express the distance in the azimuthal direction (X) and the flux function (ψ) direction (Z), respectively, with the origin located at the end of the rod which touches the surface of the hoop. This model support is retractable from the confinement region so that experiments with and without the model support can be made and compared immediately. Floating potentials and plasma densities were measured by a single Langmuir probe, and wall/hoop loss fluxes were measured by wall limiters/belt-like detectors wound around the hoop, respectively. The experiment was carried out mainly with helium plasma produced by microwave discharge with density, $n \sim 10^{11} \text{ cm}^{-3}$, and electron temperature, $T_e \sim 2 \text{ eV}$.

Figure 7 shows spatial variations of floating potential in the azimuthal direction across the model support, where a) is obtained at $Z = 16 \text{ mm}$ outside the separatrix and b) at $Z = 6 \text{ mm}$ inside it, respectively. Considering the average grad B drifts, these potential steps, which show good symmetry with respect to both the spatial position and the polarity

of the magnetic field, indicate that a charge separation occurs across the model support.^{3,4} By scanning in the Z direction, the potential variation along the model support is obtained as shown in Fig. 8. Note that in Fig. 8 the potential variations ΔV resulted from the insertion of the model support are shown. This result also indicates the charge separation in the azimuthal direction. The influence of the model support on plasma loss fluxes is shown in Fig. 9. In this figure Γ_s and Γ_o represent the loss fluxes with and without the model support, respectively, and the ratio Γ_s/Γ_o shows the change in the loss fluxes resulted from the insertion of the support. As seen in the figure, the loss is enhanced appreciably by the support on one side of it depending on the polarity of the magnetic field (see also Fig. 6); for example, if the polarity is positive (+B), the enhancement of the hoop loss is stronger at B than at A, and it is reversed as the polarity is reversed. The same is true for the wall loss (L and M), but the enhancement of the loss to the hoop and the wall occurs reciprocally with respect to the azimuth of the model support, or the stronger enhancement of the plasma loss occurs in the downstream region of the support in terms of the ion grad B drift (see Figs. 6, 7 and 9). The observed behaviour of the plasma loss cannot be explained by the charge separation electric field only. Since the electric field resulting from the charge separation produces an $E \times B$ drift in the ψ direction away from the high-density region on both sides of the separatrix near the support, the plasma loss to the hoop and the wall will be enhanced simultaneously. An additional azimuthal electric field may be required in the vicinity of the support to explain the observed behaviour of the plasma loss. Careful measurements of the floating potential across the model support were carried out near the separatrix where no potential perturbation due to the charge separation exists. The result is shown in Fig. 10. As seen in the figure, the floating potential in the vicinity of the support has been found slightly less negative on the separatrix independently of the magnetic field polarity. This indicates an additional azimuthal electric field near the support. The existence of this electric field is supported by a radial shift of density profile near the support as shown in Fig. 11. The direction of the shift coincides with the direction of the $E \times B$ flow produced by the observed electric field and the poloidal magnetic field. This type of shift of density profile has also been observed in a previous experiment made with an additional error field.²

Combining these observations described above, a schematic picture of the induced convection by the model support can be obtained consistently as shown in Fig. 12, where the equipotential contours represent the potential perturbation resulted from the model support. It must be emphasized here that the total plasma loss is enhanced substantially by the introduction of the model support, though the enhancement is caused by a rather asymmetric flows.

IV. Discussion

The possible causes of the observed anomalous plasma loss in JFT-1 are: (1) some kinds of field errors; (2) convective cells; (3) fluctuations. As mentioned in section II, the effect of field errors produced by inhomogeneity in the induced wall currents on the plasma confinement seems not to be the major process in JFT-1. The reason why this type of field errors has no significant effect on the plasma confinement has not been made clear. A possible explanation of this may be as follows. In the hexapole flux configuration of JFT-1, the mirror ratio of the magnetic field in the typical confinement region is 5-10, and the plasma is considered to be collisionless (ion mean free path ~ 30 m/ typical length of closed field line ~ 0.8 m). Trapping of ions in the mirror therefore may well be expected. This trapping process may prevent ions from spiraling along the perturbed field lines across the confinement region. Other anomalous loss processes which overcome the effect of the field error, however, may not be excluded.

As to fluctuations, previous experiments² suggest that low-frequency fluctuations localized in the steep density gradients towards the wall (drift waves) are mainly responsible for the wall loss of the microwave-produced plasma in JFT-1.

Plasma convections are caused by various asymmetries in the plasma. In the present experiment, a convection produced by obstacles penetrating the plasma confinement region were investigated. A similar experiment has been made in the Wisconsin toroidal octupole.^{3,4} In the Wisconsin octupole, the model support was electrically biased, and a resulting density step across the support was measured. It is interesting to note that the density upstream from the support in terms of the ion grad B drift was lower than the density downstream on a flux shell inside the separatrix, if the support was biased near the plasma potential. This density step

was predicted by considering the conservation of particles.

In the present experiment, no bias voltage was applied to the model support, but direct measurements of plasma loss caused by the support were made and the convective flows were studied. As described in section III, an azimuthal electric field has been observed near the support, which moves the plasma in the ψ direction. If we see the density on a flux shell azimuthally around the support, the density step will also appear across the support as in the Wisconsin octupole. This density step results from the shift of the density profile which occurs in opposite directions with respect to the azimuth of the support, and is in qualitative agreement with the observation made in the Wisconsin octupole.

A quantitative estimate of the plasma loss due to the actual hoop supports is difficult to make. Experimentally, the observed enhancement of the losses by the model support is at most a factor of 2 (Fig. 9). The support-induced convection may not be sufficient to explain the observed anomaly in the plasma loss in JFT-1.

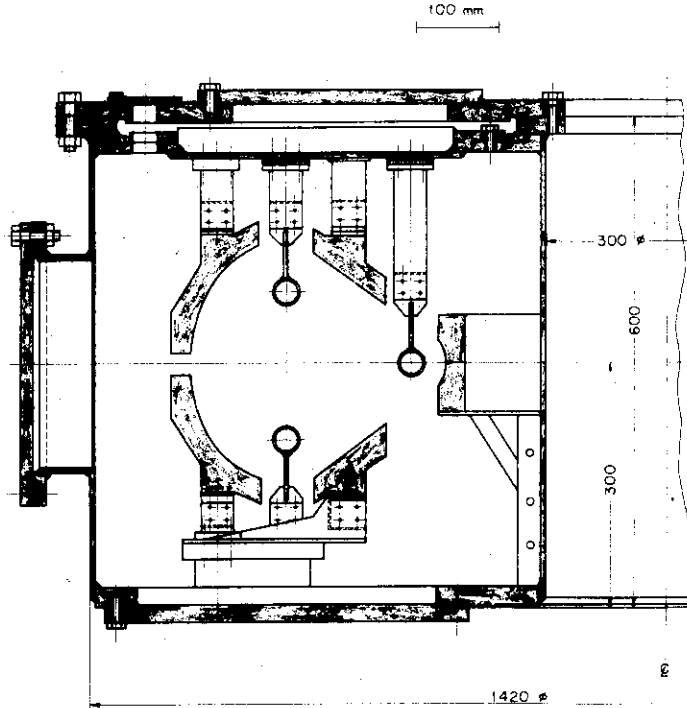
In summary, the plasma confinement time in the JAERI hexapole is limited apparently by the loss to the supports at higher magnetic fields. Anomalous losses are caused by the support-induced convection and fluctuations, but there still remains quantitative uncertainty.

References

1. S. Tamura, et al., in Plasma Physics and Controlled Nuclear Fusion Research (International Atomic Energy Agency, Vienna, 1971), Vol. I, p. 75.
2. S. Tamura, et al., in Proceedings of the Fifth European Conference on Controlled Fusion and Plasma Physics, Grenoble, August 1972, Vol. I, p. 94; S. Arizono, et al., JAERI-M 5029 (October, 1972).
3. H. Forsen, et al., in Plasma Physics and Controlled Nuclear Fusion Research (International Atomic Energy Agency, Vienna, 1969), Vol. I, p. 313.
4. J. A. Schmidt and G. L. Schmidt, Phys. Fluids 13, 1351 (1970).

Figure captions

- Fig. 1. Cross-sectional view of the JAERI hexapole with a conducting shell.
- Fig. 2. Azimuthal variation of loss flux to the outer hoop. The loss flux is measured by belt type detectors used as a single Langmuir probe.
- Fig. 3. (a) Overall confinement time $\tau = \left(\frac{1dN}{Ndt}\right)^{-1}$ vs. magnetic field strength. Time variations of plasma density are estimated from the support loss current.
 (b) Perpendicular confinement time $\tau_{\perp} = \tau \frac{\Gamma_{\parallel} + \Gamma_{\perp}}{\Gamma_{\perp}}$, where Γ_{\parallel} and Γ_{\perp} are the parallel and the perpendicular loss fluxes, respectively.
- Fig. 4. Effective diffusion coefficient $\langle D \rangle$ obtained by the relation $\Gamma = \langle D \rangle \frac{dN}{dx}$. $\langle D_B \rangle$ indicates the Bohm diffusion coefficient.
- Fig. 5. Loss ratio vs. magnetic field strength.
- Fig. 6. Experimental arrangement for model support experiment. The origin of the local co-ordinates (X, Z) is set at the contact point of the model support with the hoop. The separatrix ψ_s lies at Z = 11 mm.
- Fig. 7. Variation of floating potentials across the model support; (a) Z = 16 mm, outside the separatrix, (b) Z = 6 mm, inside the separatrix.
- Fig. 8. Variation of floating potentials along the model support at X = -5 mm. ΔV_f is defined by $\Delta V_f = V'_f - V_f$, where V'_f/V_f are the floating potential with/without the model support, respectively.
- Fig. 9. Enhancement of loss fluxes by the model support. Γ_s and Γ_0 are the loss fluxes with and without the model support, respectively. The location of loss collectors is shown in Fig. 6.
- Fig. 10. Variation of floating potentials near the model support on the separatrix (Z = 11 mm).
- Fig. 11. Density profiles at X = -5 mm along the model support.
- Fig. 12. Schematic diagram of support-induced convection. Arrows indicate the direction of the enhanced flow. Contour lines represent the enhanced potentials ΔV_f .



JFT-1
TOROIDAL HEXAPOLE
AUGUST 1972

Fig. 1.

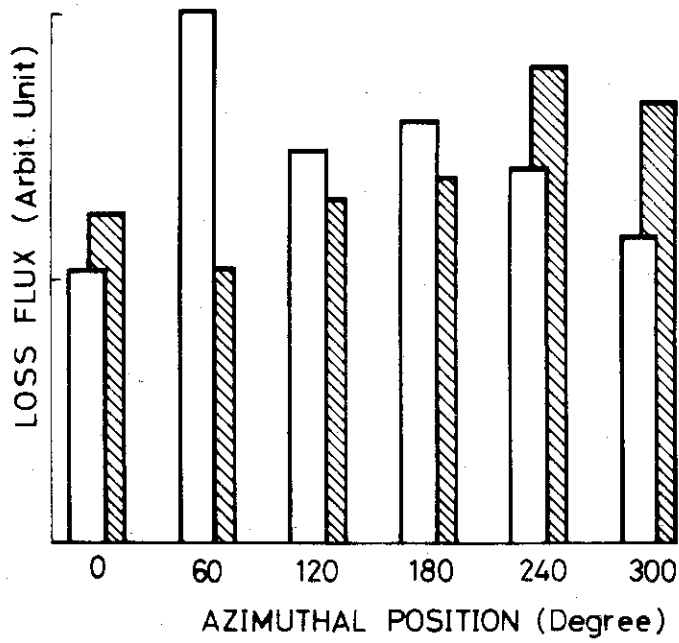


Fig. 2.

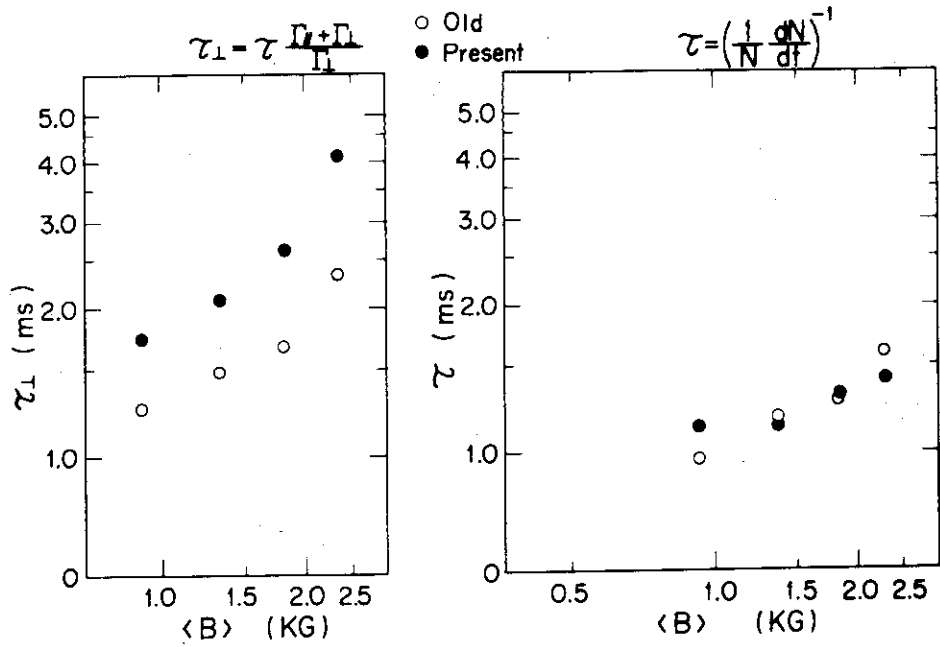


Fig. 3.

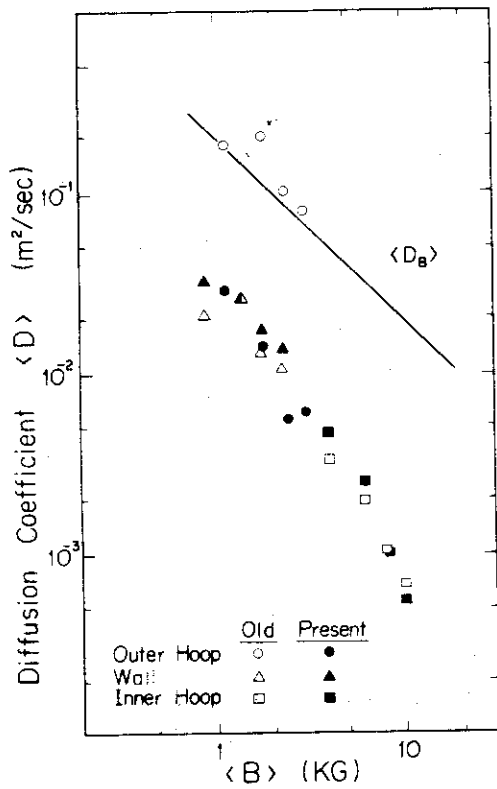


Fig. 4.

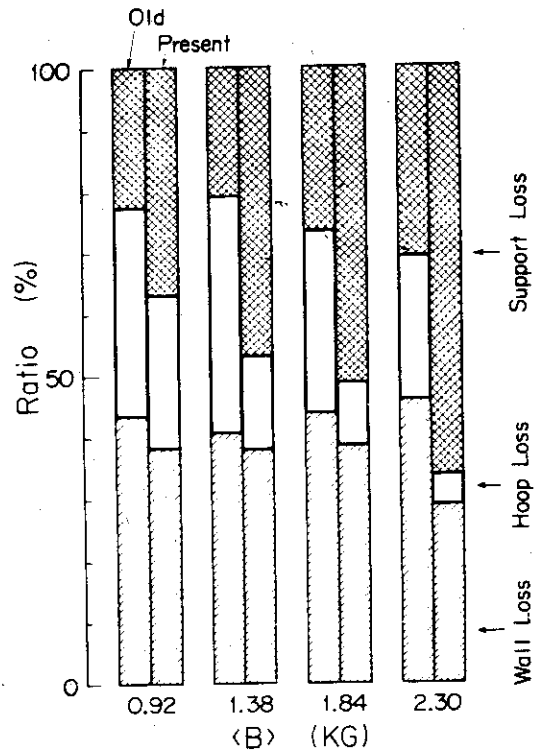


Fig. 5.

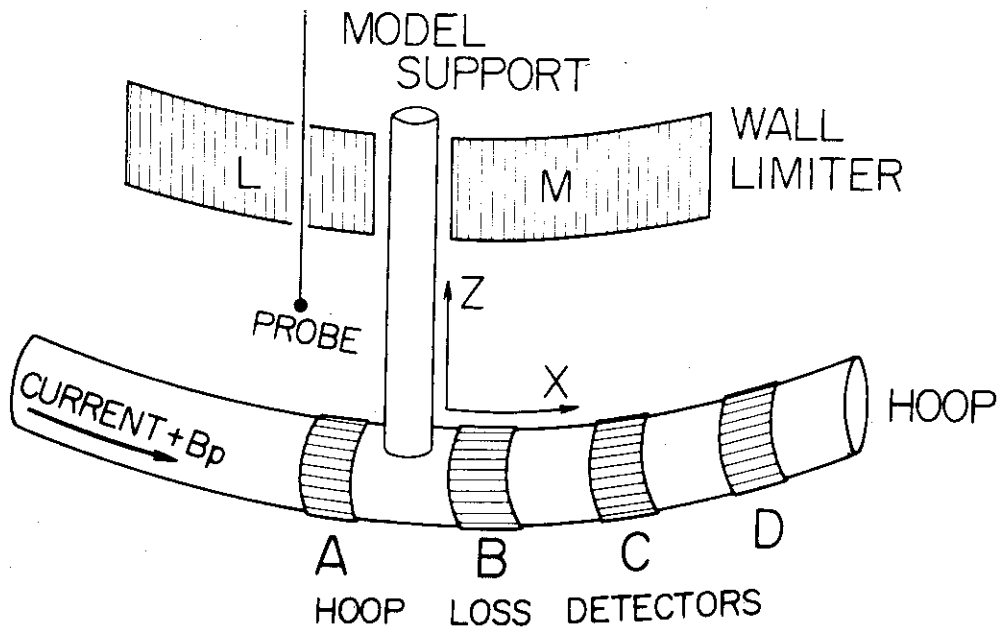


Fig. 6.

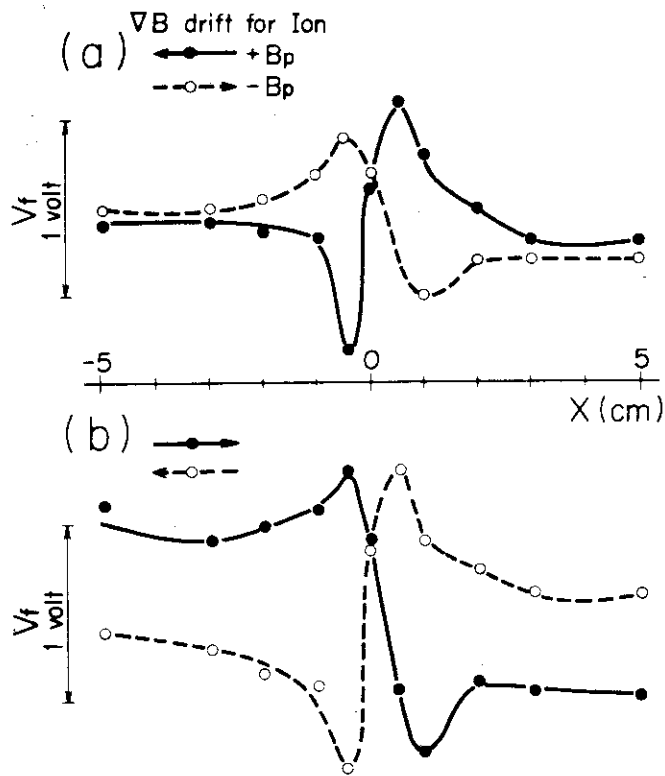


Fig. 7.

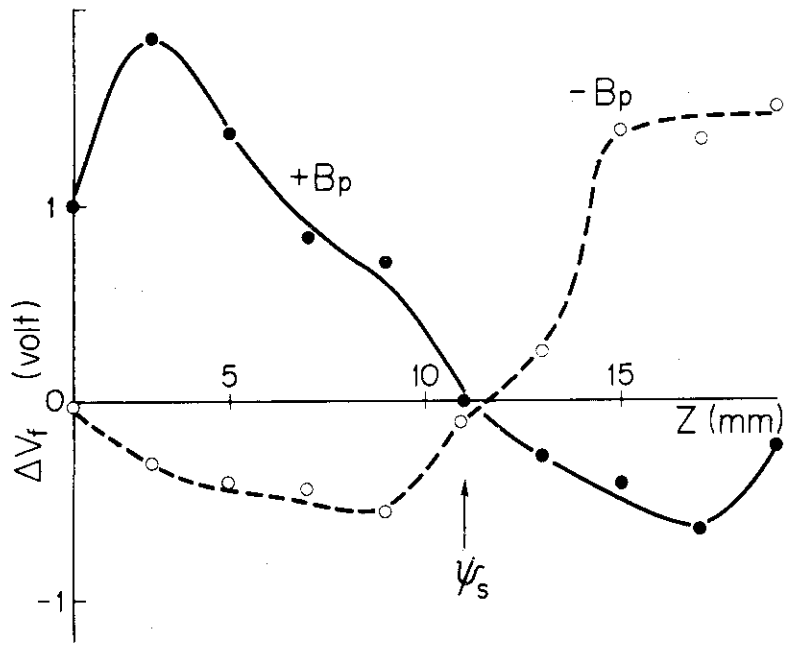


Fig. 8.

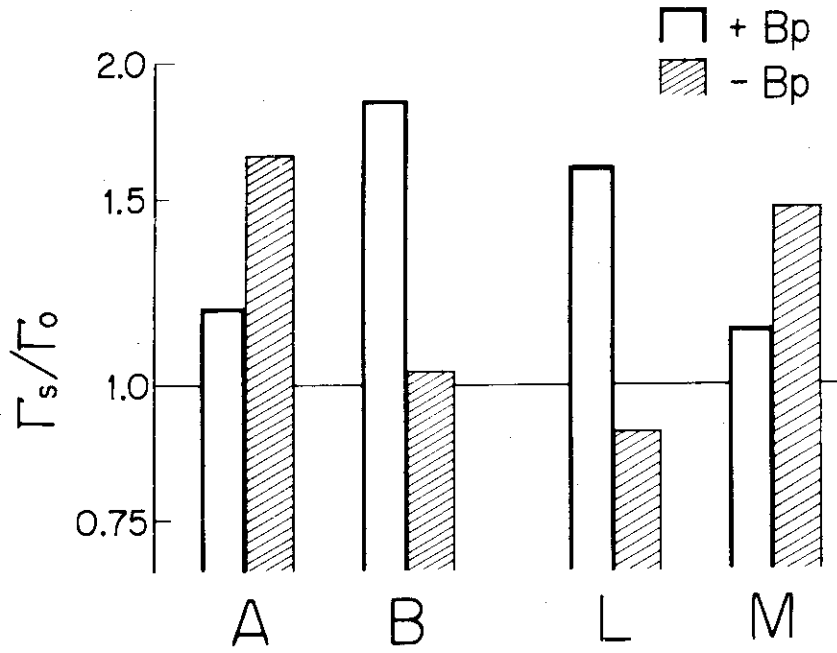


Fig. 9.

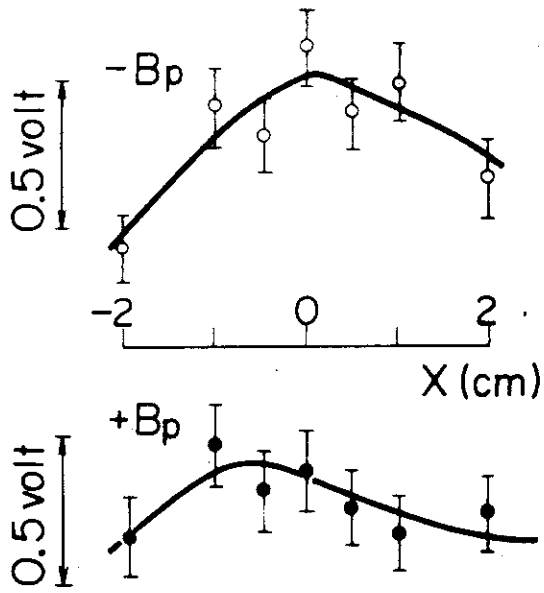


Fig. 10.

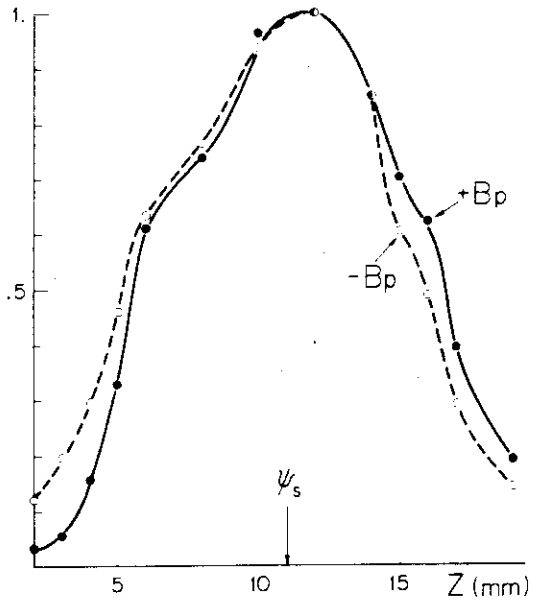


Fig. 11.

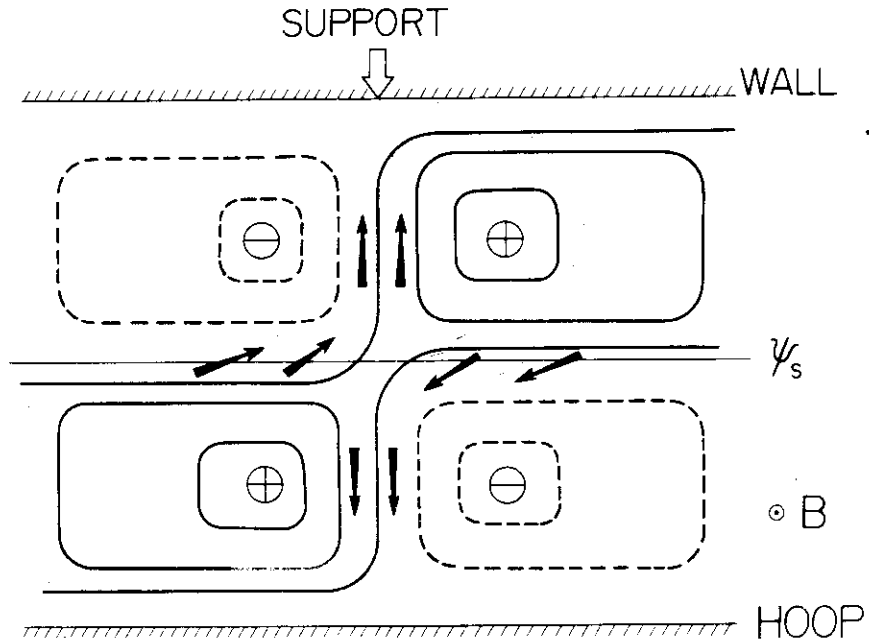


Fig. 12.